Threshold Angular Distributions of $(e,2e)$ Cross Sections of Helium Atoms

J. Botero[a] and J. H. Macek

Department of Physics and Astronomy, University of Tennessee, Knoxville, Tennessee 37996 and Oak Ridge National Laboratory, Oak Ridge, Tennessee 37831

(Received 25 October 1991)

Cross sections for the electron-impact ionization of helium atoms in a coplanar symmetric geometry are computed by including in the Coulomb-Born approximation a normalization factor which approximately incorporates electron-electron interactions in the final-state wave function. This approximation yields excellent agreement with recent experimental observations at impact energies between 0.5 and 5 eV above the ionization threshold. It is shown that the angular distributions given by the present theory are in agreement with Wannier's threshold theory.

PACS numbers: 34.80.Dp

Electron-impact ionization of atoms is a focal point of the study of the fundamental problem of few particles interacting via Coulomb forces, since it involves the simultaneous escape of two electrons in the Coulomb field of an ion [1,2]. Furthermore, when these processes occur near threshold, electron correlation effects are known to dominate [3]. Coincident detection of the outgoing electrons severely tests our theoretical understanding of these phenomena. Experimental techniques now allow measurements of the triple differential cross section (TDCS) at energies as low as 25.1 eV in helium, just 0.5 eV above the ionization threshold [1,4–6]. Theoretically, Wannier [3] showed that the electron-electron interaction was essential to obtain the correct energy dependence of ionization cross sections at threshold [7–12]. There has been no success, however, in connecting the TDCS near threshold to structures at intermediate energies. Byron and Joachain [2] showed that in order to explain some features of the TDCS of helium in coplanar symmetric geometry, a high-order approximation was required, but second-order Born approximations failed to reproduce the double peak structure of the TDCS at intermediate energies (200–500 eV) [13,14]. Distorted-wave calculations [6,15,16] have been very successful in reproducing most of the features of the TDCS at intermediate energies, down to about 100 eV. Recent work has considered these theories in the threshold region [12]. While such theories cannot reproduce the Wannier energy dependence, they provide insights into the mechanisms responsible for specific features of the angular distributions. We apply a new perturbation expansion where the electron-electron interaction is treated in first order [17,18] to the calculation of the TDCS for electron-impact ionization of helium in coplanar symmetric geometry in the threshold region.

In a recent paper [6], experimental results for coplanar $(e,2e)$ cross sections in helium at low energies were reported, which complemented an earlier work near threshold by Selles, Huetz, and Mazeau [5]. We present here an improved final-state Coulomb-Born approximation (ICBA) that reproduces remarkably well the experimental angular distribution of the TDCS at the lower energies, from 30 eV down to 25.1 eV, just 0.5 eV above threshold. We compare the new approximation, the standard Coulomb-Born approximation [17,18], the standard plane-wave Born approximation (PBA), and a plane-wave Born approximation including an improved final state (IPBA) with experiment. We conclude that the angular distribution of the TDCS at energies close to threshold is mainly dictated by the electron-electron repulsion, which we include in our theory through a normalization factor $N_{\mathbf{k}_{ee}}^{-}$ of the repulsive Coulomb wave function of the electron pair. Furthermore we show that the Coulomb interaction between the incoming electron and the screened atomic nucleus in the initial state, the Coulomb interaction between the outgoing and ejected electrons with the ion, and the electron-electron interaction in the final state are all required to give the correct angular distribution of the TDCS. We also show that, at the threshold, the angular distribution given by the present theory is in agreement with the angular distribution obtained by Wannier's analysis [10].

The main features of our theoretical approach are as follows. We use a perturbation theory that allows the expansion of the Coulomb T matrix in terms of an effective electron-atom potential [17,18]. In first order, the ICBA transition matrix element corresponding to ionization of a $(N-1)$-electron atom by an electron N is given by

$$T_{fi}^{(1)}=\langle N_{\mathbf{k}_{ee}}^{-}\psi_{\mathbf{K}_f}^{-}(\mathbf{r}_N)\Phi_f|V_{\rm int}|\psi_{\mathbf{K}_i}^{+}(\mathbf{r}_N)\Phi_i\rangle\,, \tag{1}$$

where $V_{\rm int}$ is the interaction potential of electron N with the target ion,

$$V_{\rm int}=-\frac{Z}{r_N}+\sum_{i=1}^{N-1}\frac{1}{r_{Ni}}\,, \tag{2}$$

with r_N the coordinate of electron N, $r_{ij}=1/|r_i-r_j|$, Φ_i and Φ_f the initial (i) and final (f) target eigenstates, and

$$\psi_{\mathbf{k}}^{\pm}(\mathbf{r})=(2\pi)^{-3/2}e^{-\pi ia/2}\Gamma(1\mp a)e^{i\mathbf{k}\cdot\mathbf{r}}{}_1F_1[\pm a,1;\pm i(kr\mp\mathbf{k}\cdot\mathbf{r})]=N_k^{(\pm)}e^{i\mathbf{k}\cdot\mathbf{r}}{}_1F_1[\pm a,1;\pm i(kr\mp\mathbf{k}\cdot\mathbf{r})]\,. \tag{3}$$

Here $a=iZ_{\rm eff}/k$, so that $\psi_{\mathbf{k}}^{\pm}(\mathbf{r})$ are Coulomb waves in an attractive potential with the arbitrary strength parameter $Z_{\rm eff}$.

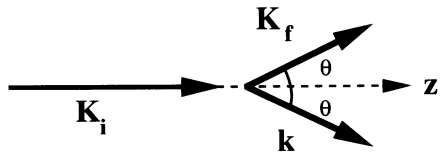

FIG. 1. Coplanar symmetric geometry for electron-impact ionization of atoms. $\mathbf{K}_i$ is the momentum of the incident electron, $\mathbf{K}_f$ and $\mathbf{k}$ are the momenta of the scattered and ejected electrons.

We consider the ionization of He by electron impact in coplanar symmetric geometry. In this geometry (see Fig. 1), the initial state consists of an incoming electron with wave vector $\mathbf{K}_i$ parallel to the z axis and a bound atomic electron in its ground state. Our model treats the helium atom as a one-electron atom, i.e., one active electron plus a passive electron whose only effect is in the screening of the projectile to give an effective charge $Z_{\rm eff}$ and in the spin statistics, and therefore we approximate the bound-state wave function by a simple hydrogenic wave function $\varphi_{1s}(r)=Z_T^{3/2}\pi^{-1/2}e^{-Z_T r}$, with Z_T equal to the screened charge chosen such that it gives the binding energy of the $1s$ electron [19]. The final state consists of two outgoing electrons with wave vectors $\mathbf{K}_f$ and $\mathbf{k}$ with $K_f=k$ and $\mathbf{K}_i\cdot\mathbf{K}_f=\mathbf{K}_i\cdot\mathbf{k}$ so that both electrons leave the atom at angles $\theta_f=-\theta_k=\theta$ which are equal in magnitude but opposite in sign. We use the method presented in Ref. [17] to compute the momentum-dependent effective charge $Z_{\rm eff}$ in the Coulomb waves of the incoming and scattered electrons.

In order to account for the electron-electron interaction explicitly in the final-state wave function, we studied the correlated three-body continuum wave function of Brauner and co-workers [20], which consists of the product of three Coulomb waves, one for each of the two-particle relative motions, and noticed that as the energy of the incoming electron decreases, the effect of the Coulomb function of the electron-electron separation in the final state is dictated mainly by the normalization constant $N_{\mathbf{k}_{ee}}^-$ with $\mathbf{k}_{ee}=\frac{1}{2}(\mathbf{K}_f-\mathbf{k})$. Consequently, we include this normalization constant of the final-state wave function in Eq. (1). Wannier's theory furthermore shows that an additional factor $\mathcal{N}(\mathbf{K}_i)$ arises in the final-state wave function owing to the electron-electron interaction. We report in this Letter relative values of the TDCS, since our goal here is to analyze the angular distribution of the TDCS, and therefore we have set $\mathcal{N}(\mathbf{K}_i)=1$ in our calculation.

The factor $N_{\mathbf{k}_{ee}}^-$ in the final state represents the effects of the electron-electron interaction. It was shown earlier [21,22] that the influence of the Coulomb interaction between the ejected and scattered electrons in PBA arises solely in a Coulomb factor $-\pi/\{k_{ee}[1-\exp(\pi/k_{ee})]\}$, which multiplies the TDCS. On the other hand, the improved final-state approximation of Rudge and Schwartz [23] uses an effective charge in the final state which gives rise to an exponential factor $\exp(-\pi/k_{ee})$, similar to $N_{\mathbf{k}_{ee}}^-$. A similar effective charge was used recently by Pan and Starace [12].

The TDCS for the ejection of an atomic $1s$ electron with momentum $\mathbf{k}$ into the solid angle $d\Omega_k$ and for scattering of the incident electron in the direction (θ_f,ϕ_f) into the solid angle $d\Omega_f$ is then given by

$$\frac{d^5\sigma}{d\Omega_f\, d\Omega_k\, d^3k_s}=(2\pi)^4\frac{2K_f}{K_i}|T_{fi}|^2. \tag{4}$$

Details of the calculation of $T_{fi}^{(1)}$ in Eq. (1) are given elsewhere [18].

The four calculations that we compare derive from the present one (ICBA), which includes Coulomb waves for both electrons in both the initial and final states and the Coulomb factor $N_{\mathbf{k}_{ee}}^-$ in the final state. The CBA is obtained by setting $N_{\mathbf{k}_{ee}}^-=1$. The IPBA retains $N_{\mathbf{k}_{ee}}^-$ but employs plane waves for the incident and scattered electrons. The PBA employs the plane waves and furthermore sets $N_{\mathbf{k}_{ee}}^-=1$. Figures 2(a)–2(d) show the TDCS for impact energies of 30, 26.6, 25.6, and 25.1 eV, respectively, in comparison with experimental results of Refs. [5] and [6]. All curves have been normalized to 1 at their respective maximum. Notice that neither the CBA nor the PBA gives the correct shape of the TDCS, while the IPBA gives a shape similar to the experimental one but with the peak at the wrong position and without the shoulder that appears at 30 eV at an angle of 90° [see Fig. 2(a)]. The present theory (ICBA) agrees very well both in the position of the peak at all energies and in the position and relative height of the shoulder. This shoulder clearly comes from the interference between single and double collision processes [24,25], which gives the dip of the TDCS at higher energies [15,17], as shown by the fact that the position of the shoulder coincides with the position of the dip in the CBA.

The presence and exact position of a single peak at the lower energies [Fig. 2(b)–2(d)] is clearly reproduced by the theory. Note that as the energy decreases the peak moves closer to 90° and the shoulder disappears. This single peak corresponds to the peak in the normalization constant $|N_{\mathbf{k}_{ee}}^-|^2$. This is shown in Fig. 3, where we plot $|N_{\mathbf{k}_{ee}}^-|^2$ at different energies. This implies that as the energy gets closer to threshold, the angular distribution of the TDCS becomes narrower and narrower around 90°. The fact that the position of the peak is always at angles greater than 90° indicates that backward scattering is dominant at lower energies. We can understand this feature by noting that, as the energy approaches threshold, the binary-encounter peak disappears since all of the initial momentum must be transferred to the nucleus. A mechanism, electron-ion scattering, provides this transfer and is included in CBA but not in PBA. Accordingly, the CBA gives relatively larger and larger backward cross sections as the energy approaches threshold. The combined effect of the backward peak in the CBA amplitude, i.e., the peak at 180°, and the 90° peak in the electron-

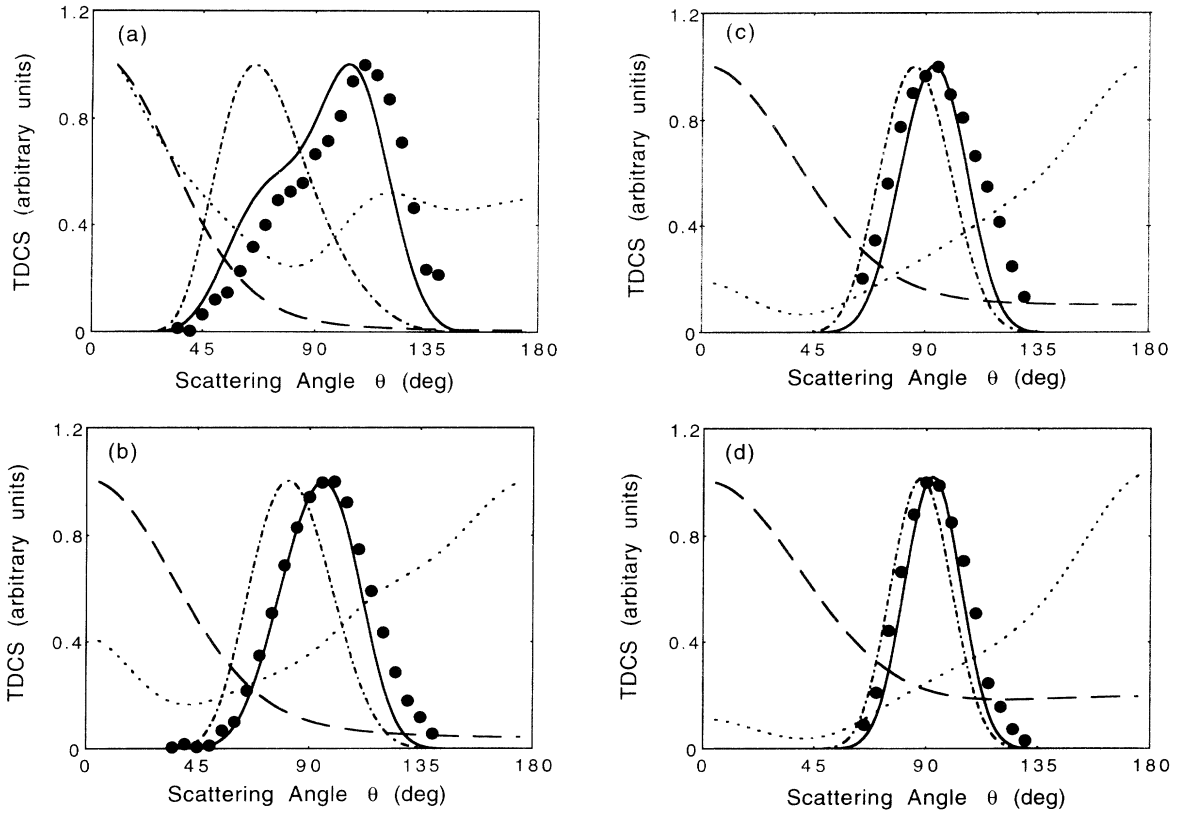

FIG. 2. TDCS for He corresponding to an energy of the incoming electron of (a) 30 eV, (b) 26.6 eV, (c) 25.6 eV, and (d) 25.1 eV. The solid line is the present calculation, the broken line is the PBA, the dotted line is the CBA, the dash-dotted line is the IPBA, and the solid dots are the experimental results from Ref. [6] in (a) and (b) and from Ref. [5] in (c) and (d).

electron factor $|N_{\mathbf{k}_{ee}}^{-}|^2$ gives a peak at the experimentally observed position at angles slightly larger than 90°. A calculation using a correlated three-body continuum wave function [20] but a plane wave in the initial state does not give the correct position of the peaks, nor does it give the correct position and relative height of the shoulder at 30 eV [26]. Our calculation shows that this is due to omission of Coulomb distortion in the initial state.

Close to threshold, the width of the angular distribution is dictated by the normalization factor $|N_{\mathbf{k}_{ee}}^{-}|^2$, which at $\gamma=2\theta\simeq\pi$ is given by [22]

$$|N_{\mathbf{k}_{ee}}^{-}|^2\simeq\exp\left(\frac{-\pi}{k_{ee}}\right)\simeq\exp\left(\frac{-\pi}{\sqrt{E}}\right)\exp\left[-\left(\frac{\pi-\gamma}{E^{1/4}\Delta\gamma}\right)^2\right], \tag{5}$$

with $\Delta\gamma=\sqrt{8/\pi}\,\mathrm{rad}=91.5°$ being the full width at half maximum of the Gaussian form derived by several authors using the Wannier threshold theory [7–11]. This shows that the angular distributions obtained within the present theory, and therefore the experimentally observed ones, are in agreement with predictions using the Wannier threshold theory [10], even though they are shifted from 90°. In essence, the angular distribution of the TDCS is given by the product of the exponential factor of Eq. (5) and a slowly varying function of energy and angle. Our results show that this function is accurately given by the Coulomb-Born approximation.

We have presented a calculation of the TDCS for

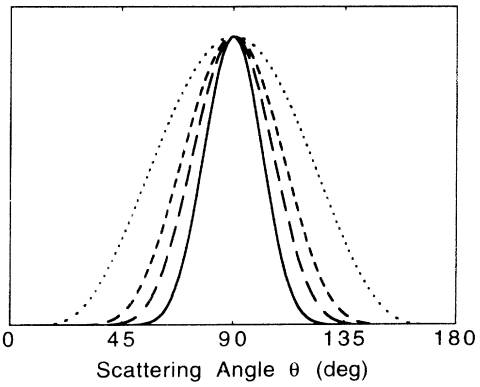

FIG. 3. Amplitude squared of the Coulomb normalization factor $|N_{\mathbf{k}_{ee}}^{-}|^2$, normalized to 1 at 90°, corresponding to an energy of the incoming electron of 25.1 eV (solid line), 26.6 eV (broken line), 30 eV (dashed line), and 100 eV (dotted line).

electron-impact ionization of helium at energies close to threshold in coplanar symmetric geometry using an improved final-state Coulomb-Born approximation. We have shown that this theory reproduces the experimental results remarkably well even at energies as low as 0.5 eV above threshold. The presence of a single peak in the TDCS, as well as the position of the peak and the dependence of its position on the energy, has been reproduced by the theory. These features have been shown to stem primarily from the electron-electron interaction in the final state, which effectively weights the double-peak structure of the TDCS in the CBA, and becomes the dominant element at energies close to threshold. We conclude that in order to explain the angular distribution of the TDCS it is required to include the Coulomb interaction between the incoming electron and the screened atomic nucleus in both initial and final states as well as the electron-electron interaction explicitly in the final state, consistent with Wannier's threshold theory [10]. We include the latter in our theory by multiplying the final-state wave function by the Coulomb normalization factor $N_{\mathbf{k}_{ee}}^{-}$.

We thank M. Brauner for fruitful discussions and M. Cavagnero for his comments on the manuscript. This research was supported by the National Science Foundation under Grant No. PHY-8918713.

[a]On leave from Escuela Colombiana de Ingeniería, Bogotá, Columbia.

[1] A. Lahman-Benani, J. Phys. B **24**, 2401 (1991), and references therein.
[2] F. W. Byron, Jr., and C. J. Joachain, Phys. Rep. **179**, 213 (1989).
[3] G. H. Wannier, Phys. Rev. **90**, 817 (1953).
[4] H. Ehrhardt, K. Jung, G. Knoth, and P. Schlemmer, Z. Phys. D **1**, 3 (1986), and references therein.
[5] P. Selles, A. Huetz, and J. Mazeau, J. Phys. B **20**, 5195 (1987).
[6] T. Rösel, C. Dupré, J. Röder, A. Duguet, K. Jung, A. Lahman-Benani, and H. Ehrhardt, J. Phys. B **24**, 3059 (1991).
[7] R. Peterkop, J. Phys. B **4**, 513 (1971); **16**, L587 (1983).
[8] A. R. P. Rau, Phys. Rev. A **4**, 207 (1971); Phys. Rep. **110**, 369 (1984).
[9] C. H. Greene and R. A. P. Rau, J. Phys. B **16**, 99 (1983).
[10] James M. Feagin, J. Phys. B **17**, 2433 (1984).
[11] P. Selles, J. Mazeau, and A. Huetz, J. Phys. B **20**, 5183 (1987).
[12] C. Pan and A. F. Starace, Phys. Rev. Lett. **67**, 185 (1991).
[13] F. W. Byron, Jr., C. J. Joachain, and B. Piiraux, J. Phys. B **16**, L789 (1983).
[14] F. Mota Furtado and P. F. O'Mahony, J. Phys. B **20**, L405 (1988).
[15] X. Zhang, C. T. Whelan, and H. R. Walters, J. Phys. B **23**, L173 (1990); **23**, L509 (1990).
[16] D. H. Madison, Comments At. Mol. Phys. **26**, 59 (1991).
[17] J. Botero and J. H. Macek, J. Phys. B **24**, L405 (1991).
[18] J. Botero and J. H. Macek, Phys. Rev. A **45**, 154 (1992); J. H. Macek and J. Botero, Phys. Rev. A **45**, 8 (1992).
[19] D. R. Bates and G. Griffing, Proc. R. Soc. London A **66**, 961 (1953).
[20] M. Brauner, J. S. Briggs, and H. Klar, J. Phys. B **22**, 2265 (1989); M. Brauner, J. S. Briggs, and J. T. Broad, J. Phys. B **24**, 287 (1991).
[21] M. Brauner and J. S. Briggs, J. Phys. B **19**, L325 (1986).
[22] M. Brauner, J. S. Briggs, H. Klar, J. T. Broad, T. Rösel, K. Jung, and H. Ehrhardt, J. Phys. B **24**, 657 (1991).
[23] M. R. H. Rudge and S. B. Schwartz, Proc. R. Soc. London **88**, 563 (1966); **88**, 579 (1966); see also M. R. H. Rudge, Rev. Mod. Phys. **40**, 564 (1968).
[24] J. S. Briggs, Comments At. Mol. Phys. **23**, 155 (1989).
[25] C. T. Whelan and H. R. Walters, J. Phys. B **23**, 2989 (1990).
[26] M. Brauner (private communication).